Two-dimensional Coulomb gas: A Monte Carlo study

Y. Saito and H. Müller-Krumbhaar
Institut für Festkörperforschung der Kernforschungsanlage Jülich, D-5170 Jülich, Federal Republic of Germany
(Received 26 February 1980)

The two-dimensional Coulomb gas with logarithmic interaction is studied by Monte Carlo simulation. We find clear evidence for the existence of a phase transition without referring to any theory. The analysis relies on the duality between Coulomb gas and discrete Gaussian model. The transition point T_c is in excellent agreement with the Kosterlitz theory. The correlation functions support the renormalization-group results and disagree with the mean-field results.

I. INTRODUCTION

The two-dimensional Coulomb-gas and related models have attracted considerable interest due to the unusual nature of its predicted phase transition. A large number of analytical studies[1–12] and numerical simulations[13–18] were performed to give quantitative predictions about universal and nonuniversal critical parameters. Recent arguments[2,8–11] support the Kosterlitz-Thouless theory[1] (KT), that the critical exponents in the Coulomb-gas[1] (CG) and the discrete-Gaussian[2,3] (DG) model agree with the six-vertex model,[5] while in contrast variational calculations[3,4] gave exponents differing by a factor of 2.

Considering correlation functions KT[1] and other authors[8,9] use renormalization arguments together with an approximate treatment of certain fluctuations. Alternatively a considerable number of numerical studies[13–18] were performed which mostly claimed to support KT. In our opinion, however, these previous simulations (unlike simulations[19]) of ordinary critical phenomena) do not settle the question of the existence of a transition. Tobochnik and Chester[16] find exponential decay of the spin-correlation functions at high temperatures, while at low temperatures spin-wave theory is in good agreement with their data. In the latter regime, however, the vortex density is so low that an exponential decay of the spin-correlation functions, if it existed, could no longer be observable for a limited system size. For instance they had a difficulty to detect an exponential decay at a temperature $T=0.95$ higher than the critical point. In order to describe an exponential tail, one needs to consider a system with linear dimensions larger than the characteristic distance between vortices. As for the critical exponent $\tilde{\nu}$ their value $\tilde{\nu}=0.7$ lies between the values $\frac{1}{2}$ and 1 from the renormalization[8,9] and variational calculations.[3,4] We show below that there is a strong variation of the correlation length due to the noncritical effects. Because of this, Swendsen[13] originally found agreement with the mean-field transition temperature. Furthermore the results obtained by Shugard, Weeks, and Gilmer[15] (e.g., the transition point at $K=1.46$) depend on the choice of the interval over which they fit the height correlation functions to the KT theory, since they apparently did not subtract the trivial saturation due to finite-size effect.

The reason for these previous problems obviously is the small system size. If, according to KT, the vortices (or charges) are the relevant excitations, one has to have a sufficiently large vortex number near the transition point in order to have sufficient statistics. At vortex-pair densities of $\lesssim 10^{-2}$ near the transition (Refs. 14 and 16 and below) one has only a 6×6 lattice of vortex pairs in a lattice of typically[15] $N=60^2$ sites. Such a small system size is below everything that has been used[19] in ordinary critical phenomena.

Our idea now is to move charges in a CG model directly instead of single spins in an XY model,[16–18] which give rise to vortices as a result of cooperation only. Thus our method is the better the lower the charge density becomes, and only unit charges are considered in our simulation. We keep the charge positions in tables and allow for creation and annihilation of pairs and for diffusion of single charges. About 10^7 configurations in an $N=400\times 400$ lattice were produced at each temperature plus similar amounts on smaller systems for comparison. Details of the procedure are given in the Appendix.

II. COULOMB-GAS AND DISCRETE-GAUSSIAN MODEL

In this section we summarize the basic formulas concerning the duality relation between the two models under consideration. The Hamiltonian[9] of our neutral Coulomb gas is

$$\mathcal{H}_{\mathrm{CG}}=-2\pi\sum_{(i,j)\neq(k,l)}\sum n(ij)\,n(kl)\,V_N(i-j,k-l) \tag{1}$$

for a quadratic $\sqrt{N} \times \sqrt{N}$ lattice. The charge unit e and the lattice constant a are taken as unity, the charges n are integers between $\pm\infty$, with the neutrality condition $\sum_{(i,j)} n(ij) = 0$. The interaction V_N is given by the lattice Green's function

$$V_N(k,l) \equiv \frac{1}{4N} \sum_{(q_x,q_y)\neq(0,0)} \frac{1-\exp[i(q_x k + q_y l)]}{2-\cos q_x - \cos q_y} \quad , \tag{2}$$

which reduces in an infinite lattice ($N \to \infty$) and for large separation to

$$V_\infty(k,l) = (4\pi)^{-1}\{\ln[(k^2+l^2)^{1/2}] + \tfrac{1}{2}\ln 8 + \gamma\} \quad , \tag{3}$$

the usual form of the logarithmically interacting neutral Coulomb gas.[8] The constant $\mu = -\frac{1}{4}(\ln 8 + 2\gamma) \approx -\frac{1}{4}\pi$ (with $\gamma = 0.577$ being Eulers constant), can be interpreted as a chemical potential of a particle with unit charge. The Hamiltonian of the DG model[2,3] is given by

$$\mathcal{H}_{\mathrm{DG}} = J \sum_{(i,j)} \{[h(ij) - h(i+1,j)]^2 + [h(ij) - h(i,j+1)]^2\} \quad , \tag{4}$$

where the height $h(ij)$ runs over all integers between $\pm\infty$. The duality[10] relation between the two models (1) and (4) provides a relation between the temperatures: $(\pi\tilde{T})^{-1} = T/J = K$, where $\tilde{T}$ is the temperature of the CG, and T of the DG model.

The height correlation function of the DG model

$$G_N(i-k, j-l) = \langle [h(ij) - h(kl)]^2 \rangle_{\mathrm{DG}} \tag{5}$$

is related to the charge correlation function of the CG by the equation[9,10]

$$\begin{aligned} G_N(x,y) = {} & 2KV_N(x,y) - (2\pi K)^2 \\ & \times \sum_{(i,j)} \sum_{(k,l)} \langle n(i,j)n(k,l)\rangle_{\mathrm{CG}} \\ & \times [V_N(x-i, y-j) - V_N(i,j)] \\ & \times [V_N(x-k, y-l) - V_N(k,l)] \quad . \end{aligned} \tag{6}$$

Since the singularity predicted[1] at T_c is extremely weak for thermodynamic quantities, we concentrate here on the correlation functions, basically in the notation of Ohta and Kawasaki[9] (their K equals πK in our notation).

At low charge densities the behavior of the system is expected[1] to be dominated by the unit charges $n = \pm 1$. (This may be checked below.) With this approximation, the renormalization-group RG calculation[9] gives a transition temperature K_c

$$K_c = 4/\pi + 8\exp(-\tfrac{1}{4}\pi^2 K_c) = 1.48\ldots \quad . \tag{7}$$

The correlation function (5) should behave[9] (near K_c, $N \to \infty$) as

$$G_\infty(R) = \left(\frac{8}{\pi} + \frac{4C}{\pi}|t|^{1/2}\right)\frac{1}{4\pi}\ln R, \quad R \gg 1 \tag{8}$$

for $t \geq 0$ where $t \equiv (T - T_c)/T_c$, and

$$(C/\pi)^2 = [2(K_c - 4/\pi) + \pi^2/2(K_c - 4\pi)^2]K_c$$

giving $C = 3.025\ldots$.

Below T_c, the correlations (5) should saturate[9] as

$$\begin{aligned} L^2 &\equiv \lim_{R\to\infty} G_\infty(R) \\ &\cong \frac{2}{\pi^2}\ln\xi \cong \frac{4}{\pi C}|t|^{-1/2} \equiv L_{\mathrm{RG}}^2 \quad , \end{aligned} \tag{9}$$

where ξ is the correlation length of height variables in the DG model. The two regions, below or above T_c, thus are characterized by saturation or logarithmic divergence of the correlation functions $G_\infty(R)$ for large R. In contrast to ordinary critical points, where the transition is marked by peaks in certain functions, the critical point here is only the boundary between two regions of asymptotically different behavior. This makes it much harder to locate the transition point without referring to a quantitative theory.

Two minor corrections to the above formulas will be useful for the interpretation of our data. First, at low temperatures $K \to 0$, the moment L^2 in the DG model behaves[14] as $L^2 \sim 4\exp(-4/K)$. We may construct a simple rational multiplier which leaves the renormalization form (9) unchanged near K_c but gives the correct asymptotic form for $K \to 0$, and we define a "reduced" moment $\tilde{L}^2$:

$$\tilde{L}^2 = [1 + (e^{4/K} - e^{4/K_c})/\pi c]^{-1} L_{\mathrm{RG}}^2 \quad . \tag{10}$$

Second, for large distances R we cannot expect a logarithmic divergence of $G_N(R)$, Eq. (8), due to the finite size of our model. On the other hand, we know how the finite size affects another closely related [Eq. (6)] function: The interaction potential $V_N(R)$, Eq. (2), in a finite system is no more simply logarithmic, but feels the finite size. We show this effect in Fig. 1, where one also observes the anisotropy for the finite-size system. For a $N = 60^2$ system, for example, finite-size effects start to become visible around $x \approx 10$, for a 400^2 system around $x \approx 60$.

We may expect that a very similar finite-size effect will occur in $G_N(R)$. In Eq. (6), we see that the first term is directly proportional to $V_N(x,y)$, while the second term also contains $V_N(x,y)$ in a more complicated manner. Therefore, plotting $G_N(R)$ vs $V_N(R)$ instead of $\ln(R)$, the trivial finite-size effect from the first term of Eq. (6) is cured. We thus may expect very little finite-size effect to be left. In particular, if we now find saturation of the correlations at large values of $V_N(R)$ it will be the physical saturation related to the phase transition rather than a trivial finite-size effect.

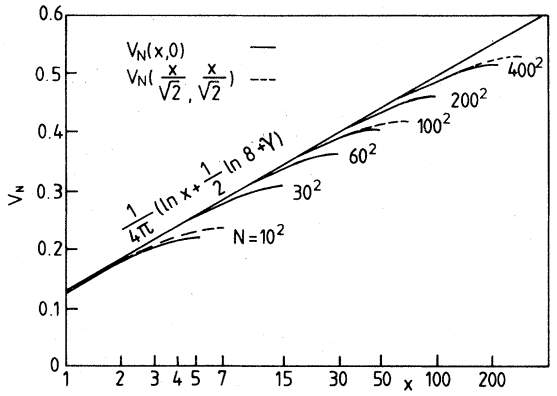

FIG. 1. Two-dimensional lattice Green's function V_N vs logarithm of distance x for various system sizes N. The continuous curve is the value for the axial direction $V_N(x,0)$ and the broken curve for the diagonal direction $V_N(x/\sqrt{2},x/\sqrt{2})$. Both of them show logarithmic behavior, Eq. (3), for intermediate distances, but there is saturation for large distances due to the finite-size effect.

III. RESULTS AND DISCUSSION

In this section we give the results of the simulation in three parts. First, we discuss the thermal properties, energy, and specific heat, then we present particle densities and correlation functions directly in the CG system, and finally we discuss the phase transition in terms of the dual DG model.

Figure 2 shows the energy E plotted versus temperature $K=T/J$ of the discrete Gaussian model dual to the CG. This energy is related to energy E_{CG} of our Coulomb gas by[18]

$$E=[\tfrac{1}{2}(1-N^{-1})-E_{\mathrm{CG}}/\tilde{T}]T \quad . \tag{11}$$

This plot allows for a direct comparison with Swendsen's results on the DG model.[13,14] We note that even though we only consider unit charges, our results for all system sizes agree precisely with Fig. 1 of Ref. 14. Since the energies in our case are due to long-range interactions, they depend sensitively on the number of particles and on correlations between particles. We, therefore, consider this agreement to be an excellent test for the correctness of our simulation procedure, for convergence to equilibrium and a justification for using unit charges. The next plot, Fig. 3, shows the specific heat (again in the DG frame) versus K. The data agree well with Refs. 13 and 14, and the remaining fluctuations do not show a systematic size dependence as the previous calculations[13,14] on smaller DG lattices.

In Fig. 4, we show the concentration c_p of charge pairs per lattice site plotted versus temperature $K=1/(\pi\tilde{T})$, where $\tilde{T}$ is the temperature of the CG. From Eq. (3) follows the Kosterlitz prediction $c_p\sim\exp(-2\mu/\tilde{T})$ for $\tilde{T}\to 0$ $(K\to\infty)$. In our units

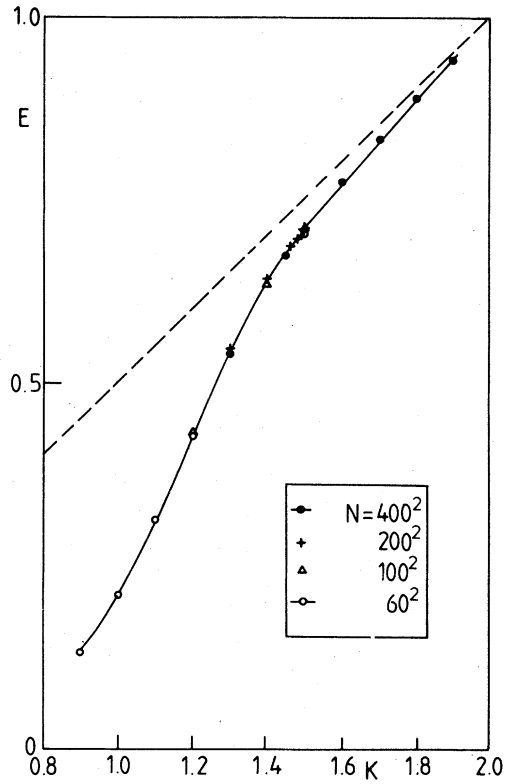

FIG. 2. Energy per site of the DG model vs temperature K. There is no observable size effect, and the result agrees with that of Swendsen (Ref. 14).

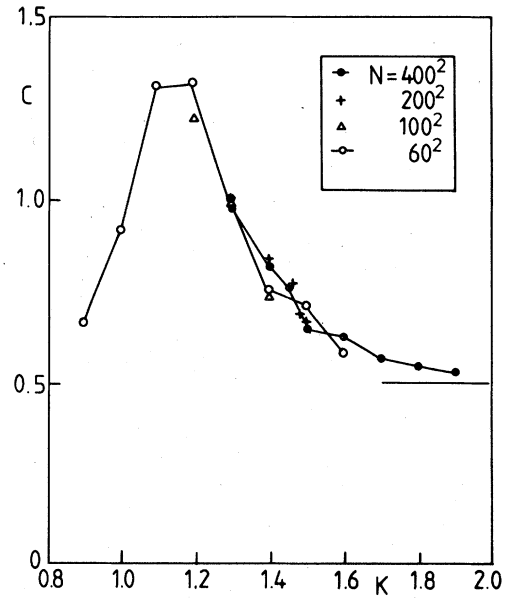

FIG. 3. Specific heat per site of the DG model vs temperature K. The maximum of the specific heat is found at a K value below the RG transition temperature $K_c\sim 1.48$ and also below the mean-field transition temperature (Refs. 3 and 4) $K_c^{\mathrm{MF}}=4/\pi\sim 1.27$.

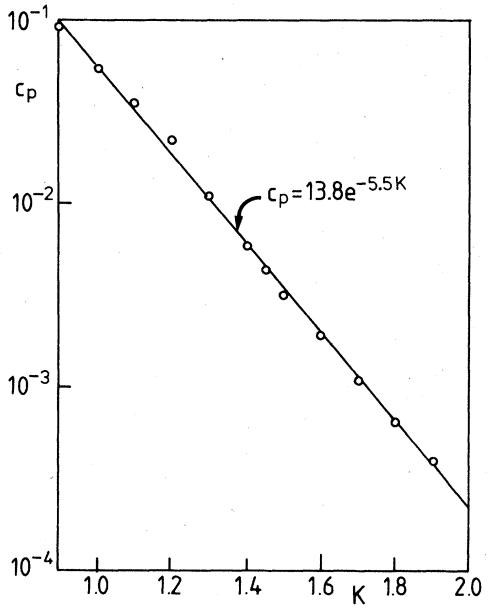

FIG. 4. Density C_p of oppositely charged particle pairs as a function of the inverse CG temperature $K = (\pi\tilde{T})^{-1}$. The temperature dependence is of the activation type $C_p = 13.8\, e^{-5.5\,\mathrm{K}}$, and no singularity is found at both the mean-field K_c^{MF} and the RG transition temperatures K_c.

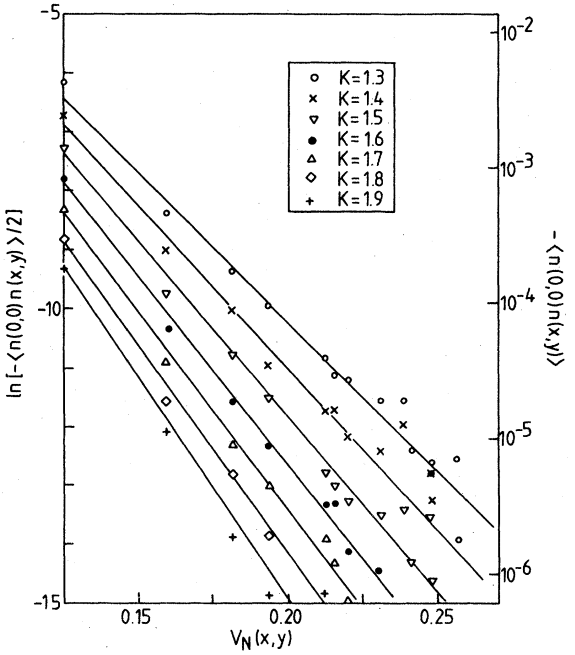

FIG. 5. Short-ranged charge correlation vs the two-dimensional lattice Green's function V_N. The lines are the low-temperature $\tilde{T}$ approximation: $\langle n(0,0)n(x,y)\rangle \sim -2\exp[-4\pi K V_N(x,y)]$, used in the RG calculation.

this means $c_p \sim \exp(-5.1\ \mathrm{K})$, while we obtain an exponent of ≈ 5.5 K. This slightly higher value may be attributed to the presence of more-distant-neighbor pairs, which require more energy. This is another check for the correctness and convergence of the calculation. Note that near the predicted transition point, we find no obvious anomaly in the temperature dependence of the pair concentration. This agrees with the observation found in the XY model[16] at smaller system size.

The next plot, Fig. 5, shows the short-range charge-charge correlation. Because of the attraction between opposite charge, the correlation is expected to be basically negative. In order to minimize the effect of the lattice anisotropy, we plot the log of the correlation function versus $V_N(x,y)$ rather than versus $\ln[(x^2+y^2)^{1/2}]$. The lines are the assumption used in the renormalization calculation.[8,9] They come from the low-temperature ($\tilde{T}\to 0$) result,[8] respectively, $K\to\infty$,

$$\langle n(0,0)n(x,y)\rangle \cong -2\exp[-4\pi^2 K V_N(x,y)]\ , \qquad (12)$$

which basically means a power-law decay as a function of distance [see Eq. (3)]. Obviously this prediction is confirmed by our calculation to a high degree of accuracy, even including the prefactor, over the whole "critical" range of temperatures. Of course, we cannot discriminate between a power-law or exponential decay (which would indicate a phase transition) by looking only at these short-ranged correlations. One way to look at the long-range correlation is studying the long-wavelength behavior ($q\to 0$) of the dielectric function:

$$\epsilon^{-1}(q) = 1 - 4\pi^2 K V_N(q)\langle n(q)n(-q)\rangle_{\mathrm{CG}}/N\ .$$

This is plotted versus $q/2\pi$ in Fig. 6. Here, $\epsilon(q)$ was averaged over the angle in the (q_x,q_y) plane. For $K = 1.5$, the plot indicates insulating behavior, $\lim_{q\to 0}\epsilon(q)$ is finite, while for $K = 1.2$, we see ap-

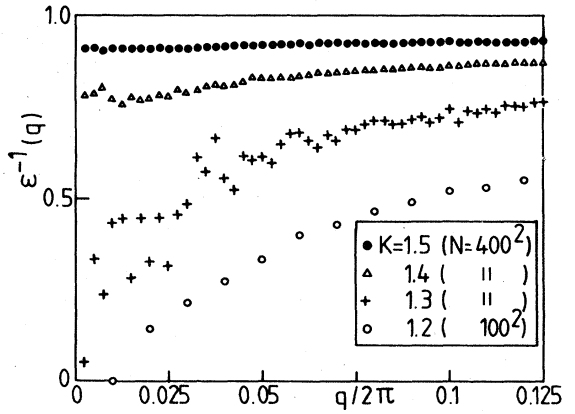

FIG. 6. Inverse dielectric function for long-wavelength q region. Finite-size effects obscure the behavior for $q\to 0$.

proximately metallic behavior: $\lim_{q\to 0}\epsilon(q)=\infty$. We cannot say anything about the exponent of the divergence in the latter case.

In the intermediate-temperature range, we observe strong fluctuations due to limited statistical accuracy. The wave number q where the inverse dielectric function $\epsilon^{-1}(q)$ takes the value half of its maximum value measures the inverse of the correlation length in the metallic phase. If the correlation length diverges exponentially as the temperature approaches some critical value $K \to K_c$ (from $K < K_c$), as predicted by the Kosterlitz-Thouless theory,[1,8,9] even the values at $K = 1.4$ might still be in the metallic range $K < K_c$. From this plot, we cannot draw a definite conclusion about a phase transition, mainly due to finite-size problems.

In order to minimize the influence of finite-size effects in the analysis, we now transform the correlations into the notation of the DG model by Eq. (6). As already mentioned in Sec. II, we then plot the function $G_N(x,0)$ vs $V_N(x,0)$, as shown in Figs. 7–9, for systems of $N = 60^2$, 200^2, and 400^2. This way of plotting eliminates the trivial size dependence of Eq. (6). Although some size effect still could be left in the second term of Eq. (6), we cannot detect any sign of a systematic size dependence in these graphs. In Fig. 7 at $K = 1.3$, one can find a small curvature but no saturation. From Fig. 7, one may

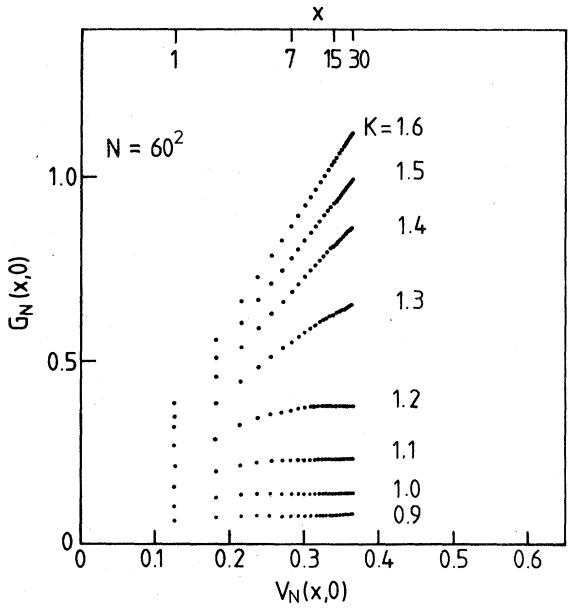

FIG. 7. Height correlation function G_N in the DG-model vs the two-dimensional lattice Green's function V_N in the x direction for the system with size $N = 60^2$. Distances in units of the lattice constant are plotted in the axis on top. Parameters are the temperature $K = T/J$. G_N at $K = 1.3$ shows only a small curvature and no saturation is observable. Previous analysis (Ref. 15) was done for $7 \leq x \leq 12$.

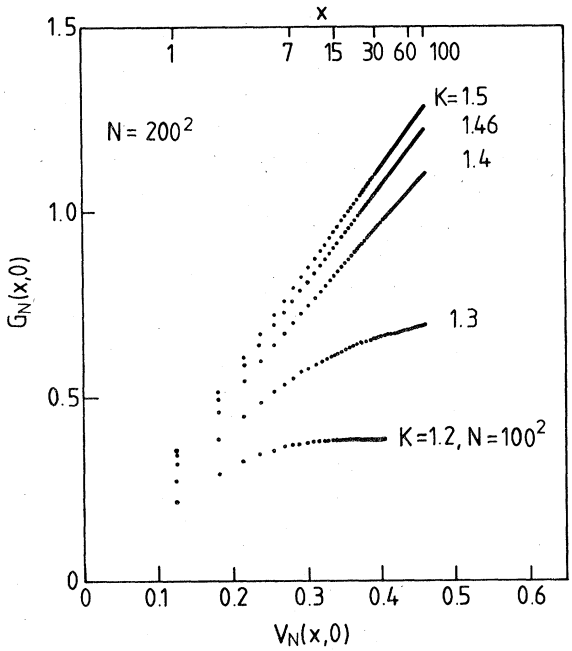

FIG. 8. Similar graph as in Fig. 7 for the larger system with $N = 200^2$. The result at $K = 1.2$ for the system $N = 100^2$ is also included.

expect a phase transition to take place between $K = 1.2$ and 1.3, but increasing the system size shows clear tendency for a saturation at $K = 1.3$. At $K = 1.5$ and larger, we cannot detect any curvature even for the largest system size.

The average distance between different particle pairs varies from ≈ 10 at $K = 1.3$ to ≈ 17 at $K = 1.5$ and thus cannot account for the difference in qualitative behavior of G_N vs V_N. We therefore argue that the curvature of the "lines" G_N vs V_N is governed by the correlation length and is associated with the saturation of the correlations at large distances. Careful inspection shows a small curvature still at $K = 1.4$. Thus we conclude that the transition temperature is at larger K value than 1.4. Our best estimate agrees with $K_c = 1.48$. Of course, like all experiments, this does not prove the existence of a phase transition in the rigorous sense. But for the first time we demonstrate the changeover from a metallic to a nonmetallic behavior in a system which is large compared to all length scales except the correlation length ξ.

On this basis, we now compare our data with the predictions from renormalization-group calculations.[1,8,9] In Fig. 10, we show the slope A of the correlations $G_N(x,y)$ taken from Figs. 8 and 9, plotted versus K for $K > K_c = 1.48$. For $K < K_c$, we give in parentheses the slopes of the tangents to the curves of Figs. 8 and 9 at the largest distances. The broken line denotes the results obtained from mean-field treatment,[3,4] the full line is the renormalization[9]

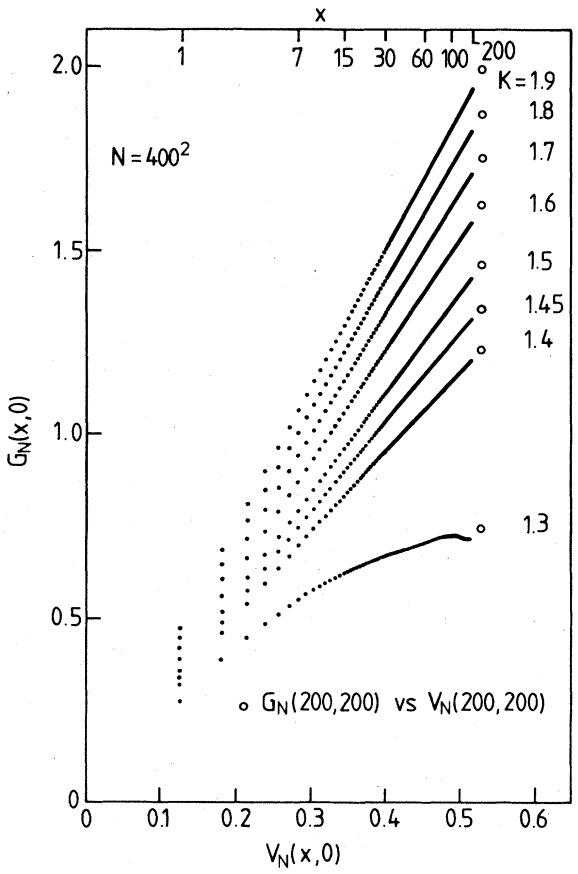

FIG. 9. Similar graph as in Figs. 7 and 8 for the largest system $N = 400^2$. The saturation of $G_N(x, 0)$ at $K = 1.3$ is now clearly seen. Apart from small fluctuations no systematic size dependence is found, compared with Figs. 7 and 8. At $K = 1.5$ no curvature can be detected, thus there is no indication for saturation in this regime.

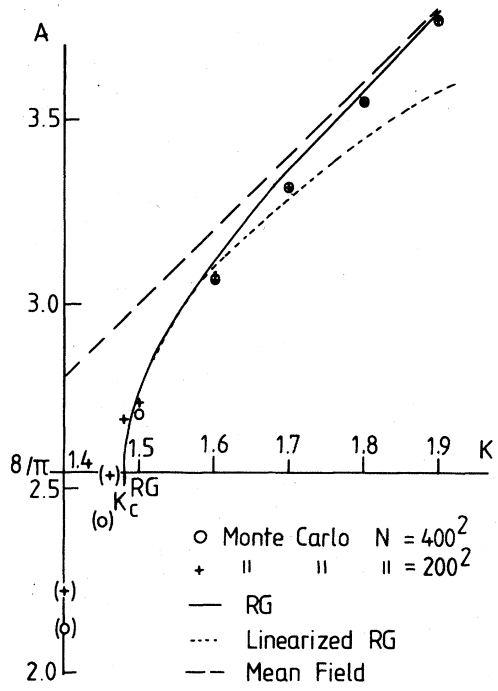

FIG. 10. Slopes A of the straight lines from Fig. 9 ($K \geq 1.5$) vs K. The slopes of the tangents to the curves of Figs. 8 and 9 at largest distance are given in parentheses. The full curve shows the renormalization (RG) result, the dashed line shows the mean-field (variational) result.

result, but here as a full solution to the renormalization equations, not just the small-$|t|$ approximation (8). We find excellent quantitative agreement between our Monte Carlo (MC) data and the renormalization results, without adjusting any parameter. The mean-field result[3,4] is clearly ruled out, since the square-root behavior is obvious.

For values $K < K_c$, we show in Fig. 11 the saturation values L^{-2}, Eq. (9), plotted versus K. We do not use the values at $K = 1.4$ and 1.45, since there we would have to extrapolate (see Fig. 9). For comparison, we give both the leading term L_{RG}^{-2}, Eq. (9), from the RG calculation[9] and the small-K-corrected values (10). We find striking quantitative agreement with this latter relation, showing that the small-K behavior is important up to the close neighborhood of K_c. The critical exponent $\tilde{\nu}$ of the correlation function, $\ln \xi \sim |t|^{-\tilde{\nu}}$, obviously cannot be determined from this calculation. One would have to calculate saturation values near $K \cong 1.45$, which leads to a necessary system size of $\sqrt{N} \approx 10^6$ lattice units (side length).

Finally, we include in Fig. 11 previous results[14] of MC simulations on the DG model (10^2 and 40^2 system). These results are better than ours for $K \lesssim 1.0$, since then in the DG model everything is short ranged. Near K_c and above, where our method is most effective, those values are not useful anymore.

To summarize, we have obtained excellent quantitative agreement with the renormalization calculations of correlation functions.[9] The mean-field results[3,4] cannot account for our data. We have set the chemical potential such that the CG and DG models are equivalent. We can also vary the chemical potential in order to investigate the critical line in an activity versus temperature plot, but this is beyond the scope of the present investigation.

ACKNOWLEDGMENTS

We thank Professor K. Binder and Professor H. U. Everts for discussions.

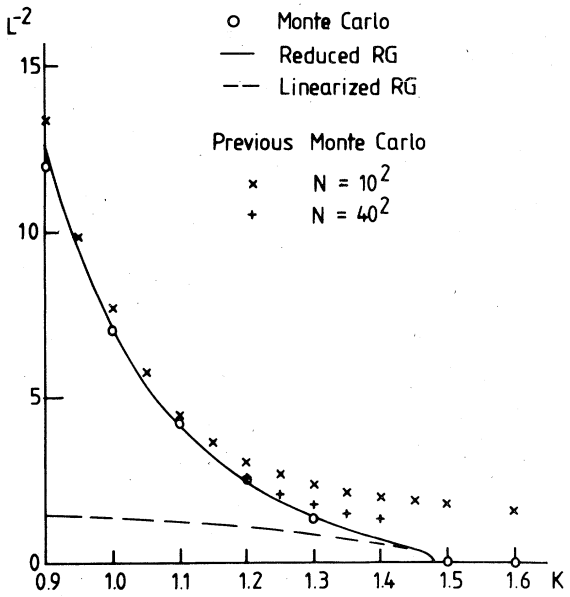

FIG. 11. Inverse saturation value L^{-2} of the correlation functions (Figs. 7 and 9) vs K. The broken line is the linearized renormalization (RG) result [Eq. (9)], the full line is our low-K corrected formula [Eq. (10)]. The low-K behavior clearly is dominating up to a temperature $K \lesssim 0.9K_c$. The predicted square-root behavior near K_c thus could only be seen in a region within 3% below K_c. Previous Monte Carlo data (Ref. 14) are included for comparison.

APPENDIX: MONTE CARLO PROCEDURE

Our Coulomb-gas system is a grand canonical ensemble, the particle number being not conserved. The simulation process then consists of a creation and an annihilation of pairs of particles with positive and negative charges and of diffusion of single particles. Thus the total charge is zero.

Since the lowest energy barrier to create a particle pair corresponds to a nearest-neighbor pair, we consider only nearest-neighbor-pair creation and its reciprocal process, nearest-neighbor-pair annihilation. Although lowest, the barrier to create a pair 2μ is still larger than the thermal activation energy $\tilde{T} = \pi K^{-1}$ near the critical point, and hence most attempts to create a pair will be unsuccessful if the normal Metropolis method is applied. Correspondingly there are not many charged particles in the system. At $K = 1.9$, 1.6, and 1.3 there are ~ 63, ~ 310, and ~ 1750 particle pairs, respectively, in $N = 400^2 = 160\,000$ system. Therefore using the Metropolis method, most of the CPU time is spent without changing the configuration.

We introduce a new method of simulation to speed up the process. In the first stage, we decide whether we try pair creation or annihilation according to a certain probability. The creation is tried with a constant probability $p_{cr}(<1)$, but the annihilation is tried with a probability p_{an}, proportional to the density $C_{+-}(\ll 1)$ of the nearest-neighboring particle pairs with opposite charges multiplied by the factor $e^{2\mu/\tilde{T}}$ $(\gg 1)$. Although C_{+-} is very small, the large factor $e^{2\mu/\tilde{T}}$ enhances the rate of annihilation trials.

In the second stage, if creation is being tried, we pick up a lattice site and one of its neighbors at random. Only if both sites are unoccupied we calculate the energy change ΔE_{cr} associated with the pair creation, and otherwise we skip to the next process. If the energy change is smaller than 2μ, the pair is created. If the energy change is larger than 2μ, the pair is created with probability $\exp[-(\Delta E_{cr} - 2\mu)/\tilde{T}]$ (≤ 1). Compared with the Metropolis method, we have shifted the energy reference from 0 to 2μ, and enhanced the creation rate by $e^{2\mu/\tilde{T}}$, which counteracts the enhancement of annihilation trials p_{an}. In order to perform the annihilation process effectively, we keep the location of the nearest-neighboring opposite charges in a table. If the annihilation is being tried, we pick up a nearest-neighboring pair at random from the table, calculate the energy change associated with the pair annihilation; $\Delta E_{an} = -\Delta E_{cr}$. If the energy change ΔE_{an} is smaller than -2μ, the pair is annihilated. If the change ΔE is larger than -2μ, the annihilation is performed with probability $\exp[(-\Delta E_{an} - 2\mu)/\tilde{T}]$ (≤ 1). With this method the enhancement of annihilation rate in the first stage and of creation rate in the second stage speeds up the total process essentially by a factor $e^{2\mu/\tilde{T}} \sim 10^2$, compared with the usual Metropolis method near the critical point.

The diffusion of positive or negative charges is performed alternatingly with creation and annihilation processes. We keep the positions of the positive and negative charges in other tables, and we pick up a particle from these tables at random. This increases the number of the diffusion trials effectively. The energy change is treated by the usual Metropolis method.

Finally we give a few comments on the "logarithmic" interaction of the Coulomb-gas system. Our interaction is not truely logarithmic but is essentially a two-dimensional lattice Green's function V_N in Eq. (2). In the simulation V_N is evaluated numerically by the "fast Fourier transform." The interaction is not divergent for large separation but it saturates as the separation approaches the system size as shown in Fig. 1, and is periodic with the period of system length;

$$V_N(k+\sqrt{N},l) = V_N(k,l+\sqrt{N}) = V_N(k,l) \quad .$$

In the usual Coulomb-gas system with truely long-ranged interaction, we have to consider the image systems periodically arranged around the original system and it is necessary to calculate the energy between the original system and all the image system by Ewald summation in addition to the interaction energy of the original system. In our case, however, the periodicity of the DG model is incorporated in the periodic potential V_N, and the interaction (1) is effective only between the particles in the original system. By this procedure we circumvent the necessity to perform explicit Ewald summation.

[1]J. M. Kosterlitz and D. J. Thouless, J. Phys. C 6, 1181 (1973); J. M. Kosterlitz, *ibid.* 7, 1046 (1974); 10, 3753 (1977).

[2]A review on the discrete Gaussian model and related models is given by J. D. Weeks, in *Ordering in Strongly Fluctuating Condensed Matter Systems,* edited by T. Riste (Plenum, New York and London, 1980). See also A. P. Young, same reference.

[3]H. Müller-Krumbhaar, in *Crystal Growth and Materials,* edited by E. Kaldis and H. Scheel (North-Holland, Amsterdam, 1977), Vol. 2, and the references cited therein.

[4]Y. Saito, Z. Phys. B 32, 75 (1978); Prog. Theor. Phys. 62, 927 (1979).

[5]H. van Beijeren, Phys. Rev. Lett. 38, 993 (1977).

[6]J. Zittartz and B. A. Huberman, Solid State Commun. 18, 1373 (1976).

[7]H. U. Everts and H. Schulz, Z. Phys. B 22, 285 (1975); H. U. Everts and W. Koch, *ibid.* 28, 117 (1977).

[8]J. V. José, L. P. Kadanoff, S. Kirkpatrick, and D. R. Nelson, Phys. Rev. B 16, 1217 (1977).

[9]T. Ohta and K. Kawasaki, Prog. Theor. Phys. 60, 365 (1978).

[10]S. T. Chui and J. D. Weeks, Phys. Rev. B 14, 4978 (1976); Phys. Rev. Lett. 40, 733 (1978).

[11]D. Amit, Y. Y. Goldschmidt, and G. Grinstein, J. Phys. A 13, 585 (1980).

[12]J. Zittartz, Z. Phys. B 23, 55, 63 (1976); 31, 63, 79, 89 (1978).

[13]R. H. Swendsen, Phys. Rev. B 15, 5421 (1977).

[14]R. H. Swendsen, Phys. Rev. B 18, 492 (1978).

[15]W. J. Shugard, J. D. Weeks, and G. H. Gilmer, Phys. Rev. Lett. 41, 1399 (1978).

[16]J. Tobochnik and G. V. Chester, Phys. Rev. B 20, 3761 (1979).

[17]W. L. McMillan (unpublished).

[18]S. Miyashita, H. Nishimori, A. Kuroda, and M. Suzuki, Prog. Theor. Phys. 60, 1669 (1978).

[19]*Monte Carlo Methods in Statistical Physics,* edited by K. Binder (Springer, Heidelberg, 1979).